Precipitation Measurement Using SIR-C
A Feasibility Study

Investigation at Nadir

Atiq Ahamad and Richard K. Moore

Radar Systems and Remote Sensing Laboratory
Department of Electrical Engineering and Computer Science, University of Kansas
2291 Irving Hill Road, Lawrence, Kansas 66045-2969
TEL: 913/864-4835 * FAX: 913/864-7789 * OMNET: KANSAS.U.RSL

RSL Technical Report 8370-2

December 1993

Sponsored by:

NASA Jet Propulsion Laboratory
Pasadena CA 91109

Grant NAS7-918, 958522

ABSTRACT

The most significant limitation of the imaging SAR in rain measurements is the ground return coupled to the rain cell. Here we report a study of the possibility of using the X-SAR and the C-band channel of SIR-C for rain measurement. Earlier signal-to-clutter calculations rule out the use of X-SAR at steeper off-vertical angles of incidence (i.e., $20 < \theta < 50$). Only rain rates > 30 mm/hr at angles of incidence > 60° showed good signal-to-clutter ratio (SCR).

This study involved calculations at vertical incidence. There is adequate signal-to-noise ratio (SNR) at vertical incidence, but the presence of high-range side-lobe levels leads to small SCR for measurement over oceans at both X and C bands. For larger rain thickness (> 2 km), the SCR gets better and smaller rain rates (> 10mm/hr) can be measured. However, rain measurements over forests seem to be feasible at nadir even for smaller rain thickness (< 2 km). We conclude that X band may be usable over the forest at vertical incidence to measure rain rates > 5 mm/hr even for shallow rain thickness and over ocean for large rain thickness.

1.0 INTRODUCTION

The detection and measurement of precipitation from space platforms is important in various meteorological applications. A precipitation detection and measurement experiment was accepted for the SIR-C/X-SAR mission. The proposed experiment will use the SIR-C /X-SAR sensors, to measure rain quantitatively for moderate to intense rain rates (> 10 mm/hr). X-SAR achieves adequate SNR at all angles of incidence for all but the lightest rains. The C-band SIR-C gets reasonable SNR at all angles for moderate to heavy rains. However, the SCR is so poor at C band that it cannot be used over any reasonable ground surface. Earlier it was concluded that it would be possible to measure rain rates in excess of 30 mm/hr at angles of incidence greater than 60°. For this study we use the backscatter method for rain-rate measurement. The backscatter algorithm is the simplest of algorithms; however its use without corrections for attenuation leads to considerable error in the rain rate estimation (Goldhirsh, 1988).

2.0 SYNTHETIC-APERTURE RADAR RESOLUTION IN RAIN

When observing a target, the maximum possible aperture that can be synthesized during time T_a for which the target is illuminated is

$$L_s = U\, T_a \tag{1}$$

where U is the platform velocity. Atlas and Moore (1987), showed that the expected Doppler spread from rain permits only a relatively short integration time. A Synthetic-aperture radar (SAR) has better resolution than a real-aperture radar only when

$$\sigma_{vs} < \frac{\lambda\, U}{6\, L_n} \tag{2}$$

where L_n is the length of the along-track real aperture, U is the platform velocity and σ_{vs} is the standard deviation of the Doppler velocity spectrum. The critical value of σ_{vs} is 3.75 m/s for X band and 6.81 m/s for C band. The SAR can use the full synthetic-aperture only when the targets in the pulse volume are correlated (i.e., their phase positions remain fixed). This means that the effective beamwidth, with rain as the target, increases with the increase in σ_{vs}, the spread of the target Doppler spectrum.

2.1 GEOMETRY

The echo power for the SAR is identical to that for the conventional real aperture radar, using the same antenna. Hence, will use the same geometry as that of real-aperture for power calculations. Fig. 1 shows the geometry for the vertical incidence. The rain volume may be

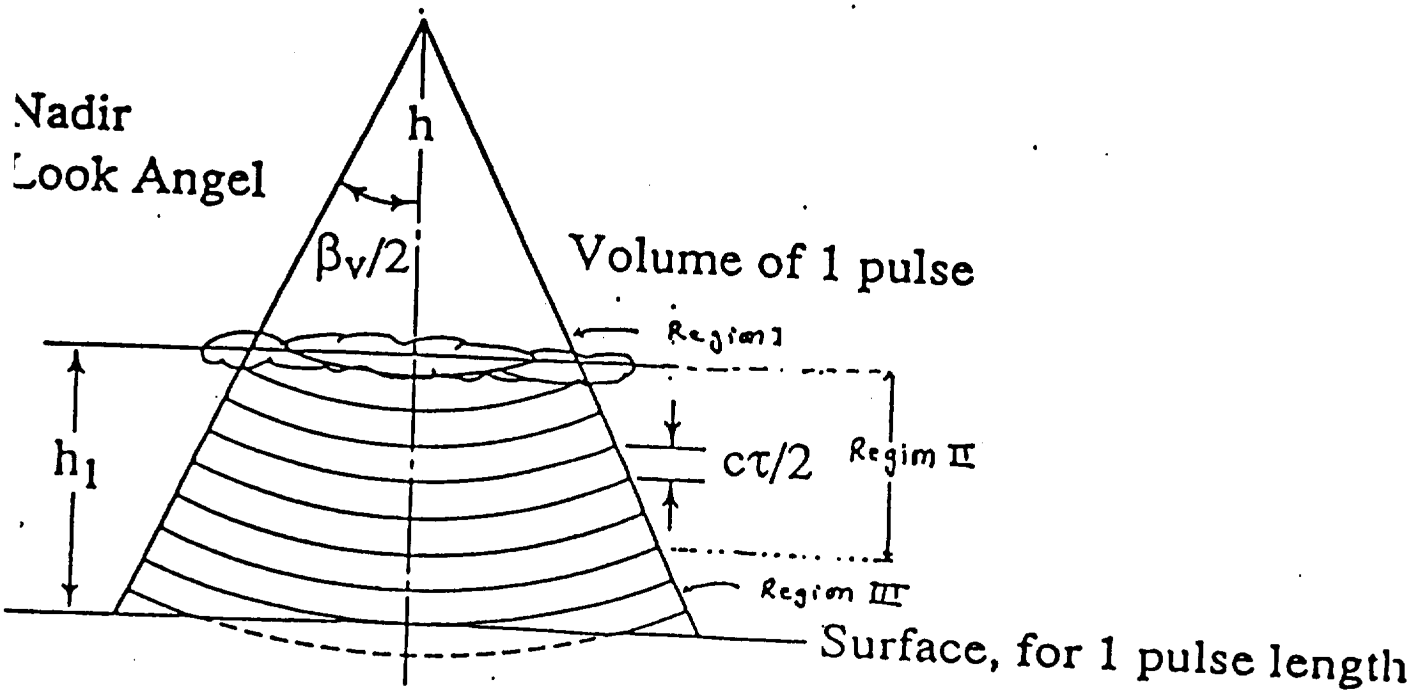

Fig.1 The geometry with the shuttle looking at nadir.

divided into three regions.

Region 1. where there is partial beam filling due to the pulse intercepting the cloud top.

Region 2. where the cells are assumed to be completely rain filled.

Region 3. where the rain cells intercept the surface.

Here we consider calculations only for those cells that are completely rain filled (ideal rain cells). The volume of these rain cells is

$$V_n = \frac{\pi}{4} \beta_h \beta_v r_R R_n^2 \tag{3}$$

where R_n is the range to the cell in question, β_h and β_v are the horizontal and the vertical beam widths, and r_R is the vertical resolution. The factor of $\pi/4$ accounts for the elliptical shape of the beam. The ground area coupled to each cell except the first can be calculated, assuming the area is approximately rectangular (see Fig. 2), as

$$A_n = 2 \beta_h R_n (x(n) - x(n-1)) \tag{4}$$

and the ground area coupled to the first cell is given by

$$A_1 = 2 \beta_h R_n x(1) \tag{5}$$

where

$$x(n) = R_n \sin(\theta_n) \tag{6}$$

$$\theta_n = \cos^{-1}(\frac{h_s}{R_n}) \tag{7}$$

and

$$R_n = h_s + n r_R \tag{8}$$

We define h_s as the shuttle altitude, R_n as the range to the particular cell in question and n as the

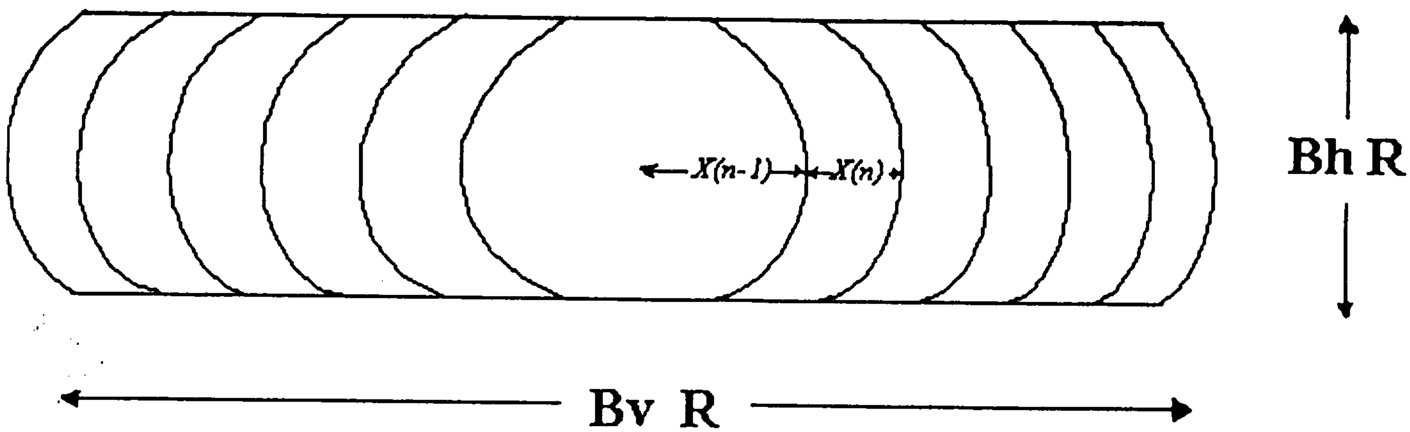

Fig.2 The geometry of the rain cells intersecting the surface, on the ground .

cell number ranging from 1 to m. To calculate m, the total number of cells coupled to the ground, we use the relation

$$m = \frac{R_s - h_s}{r_R} \tag{9}$$

where R_s is the maximum slant range to the ground (see Fig. 3)

$$R_s = \frac{h_s}{\cos(\beta_v/2)} \tag{10}$$

3.0 MODELS USED

For vertical incidence, the ocean return at X band is assumed to have a scattering coefficient σ^o of 12 dB (Schroeder et al., 1985) and forests to have a σ^o of -6 dB (Ulaby et al., 1986) . Further, due to the large magnitude of the returns, backscatter modification due to wind speeds and impinging rain drops is ignored.

Radar meteorologists have derived an empirical power law, the Z-R relationship, from the available data and Mie scattering (Battan,1973) . That is

$$Z = a\, R_r^{b_1} \tag{11}$$

where a and b_1 have been found to depend on the dropsize distribution, rain type, rain rate, frequency, and the region. Although it is clear that the Z-R relation is useful, the values of the coefficient must be selected judiciously. The coefficients differ markedly at small and large values of rain rate R_r, hence a single Z-R relationship cannot be used. For modest and small rain rates, it is resonable to select a around 300 and b_1 around 1.5 (Atlas and Moore 1987).

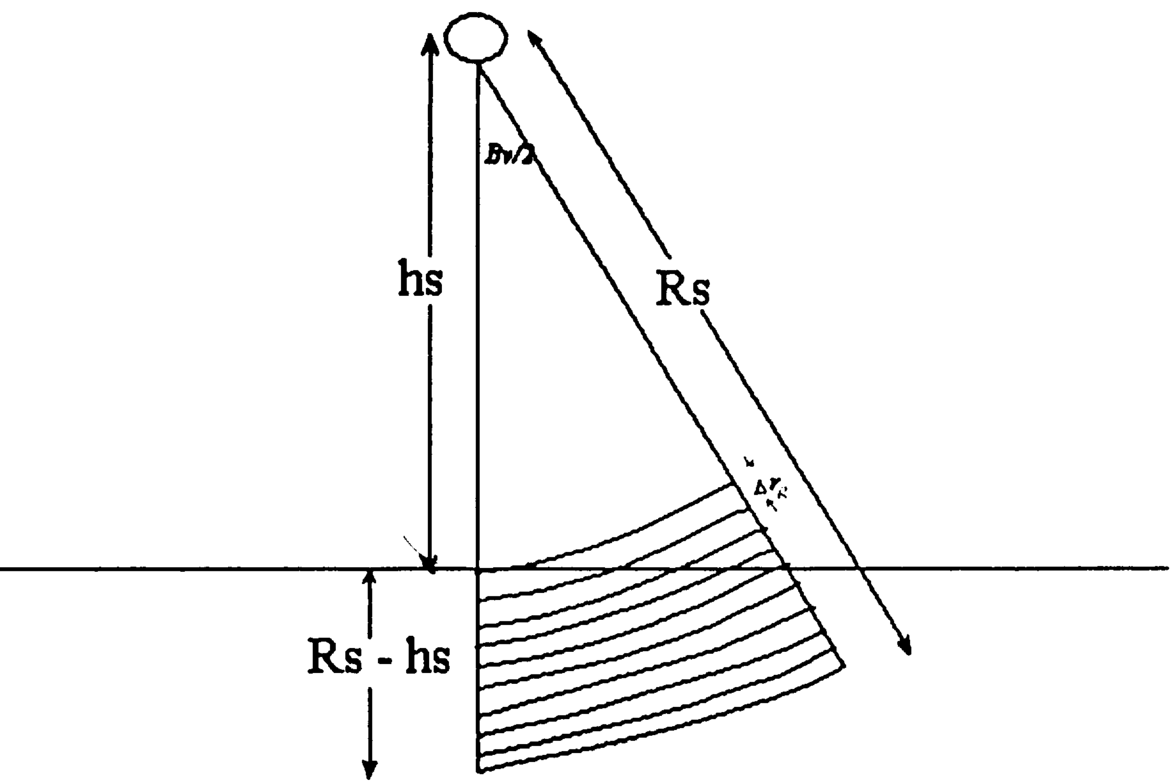

Fig.3 The geometry to calculate the number of cells coupled with the surface echo.

4.0 SIGNAL-TO-NOISE RATIO

From the basic radar equation

$$P_r = \frac{P_t\, G^2\, \lambda^2\, \sigma_v}{(4\pi)^3\, R^4} \tag{12}$$

where the variables have their usual meaning, we obtain an equation for SNR. For the vertical incidence angles, using (3) for volume of the ideal rain cells, (12) may be written as

$$SNR_n = \frac{P_t}{K\, T\, B\, F}\ \frac{G^2\, \lambda^2\, \beta_h\, c\, \tau\, \eta\, L_b\, L_s}{1024\, \pi^2\, R^2}\, K_{er}[Rr] \tag{13}$$

where

$$\eta = \frac{\pi^5\, 300\, R^{1.5}\, |k|\, 10^{-10}}{\lambda^4} \tag{14}$$

Here G is the gain, B is the bandwidth, L_s is the system loss, L_b is the signal loss due to absorption by the melting ice layer, η is the rain reflectivity, F is the receiver noise figure, and the other parameters have their usual meaning. The extinction coefficient [see Appendix I] is

$$k_{er}[Rr] = \int_{-\frac{\beta_v}{2}}^{\frac{\beta_v}{2}} e^{-2\,\alpha[Rr]\,\left(h_d\left(\frac{\cos(\theta)-1}{\cos(\theta)}\right) + h_k\right)}\, d\theta \tag{15}$$

where

$$\alpha[Rr] = \frac{b\, Rr^{\,c}}{8.66} \tag{16}$$

The value of *b* and *c* depend on the frequency used (see Table 1), h_d is the shuttle's height above the top of the rain cell and h_k is the distance of the rain cell from the rain top. Using (13) we plot the SNR in dB vs rain rate in Fig. 4.

Only calculations for the cells that are entirely rain filled are presented here. For partially

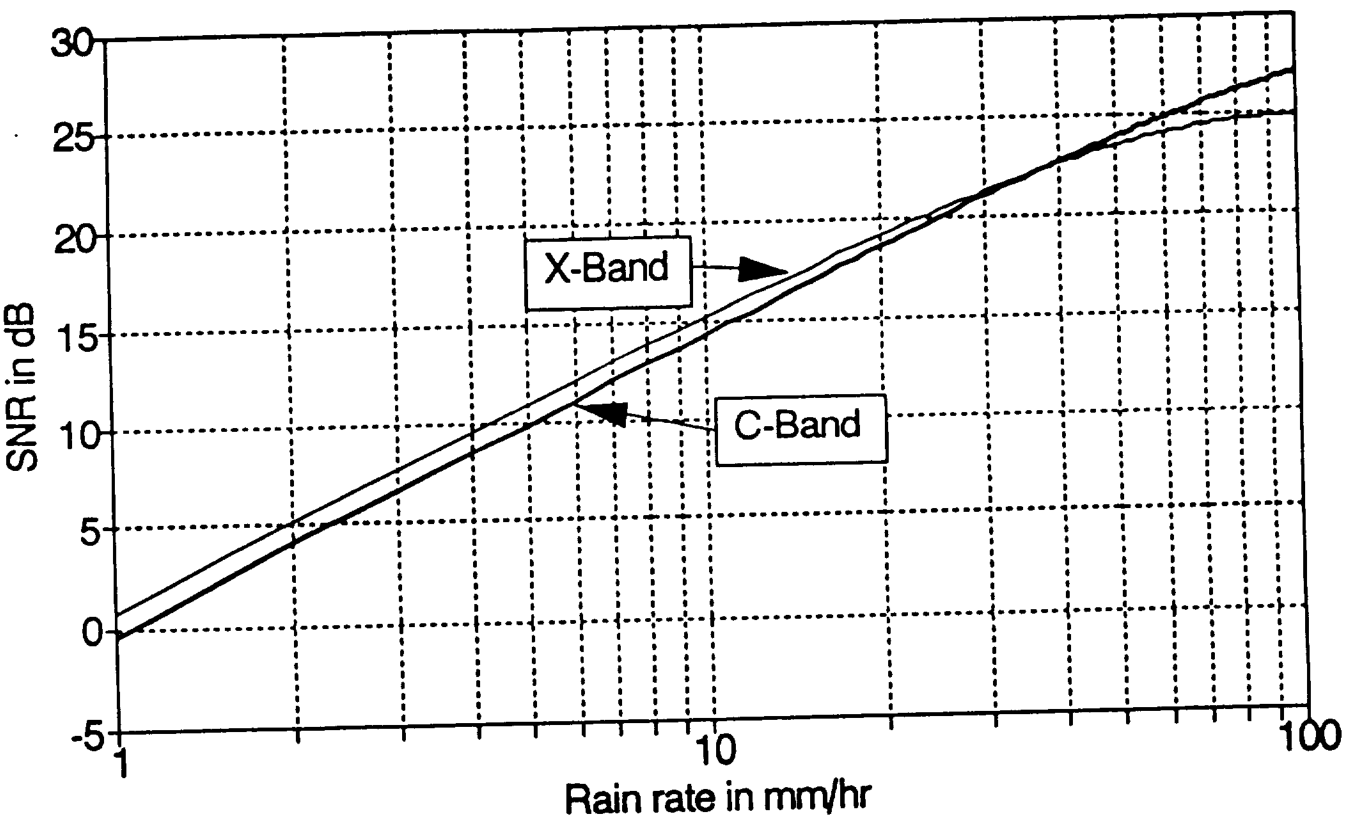

Fig.4 Plot of the SNR in dB vs Rain rate in mm/hr for vertical incidence.

rain-filled cells, the SNR decreases in proportion to the rain-filled volume.

5.0 SIGNAL-TO-CLUTTER RATIO.

The backscatter method uses the returned echo from the rain to compute the rain rate. For vertical incidence the surface returns, coupled by the sidelobes, arrive simultaneously with the desired echo and increase in magnitude as we approach cells near the surface. For the backscatter method to work, the echo from the rain should be substantially above the surface echo to allow separating them. Hence, we compute the **signal-to-clutter ratio**. This is defined as the ratio of the desired signal (rain return) to the surface return. Since the surface and the rain are excited by the same transmitter, one need not use the radar equation in its entirety.

The scattering coefficient of the rain, when λ is in centimeters, is

$$\sigma_r = \frac{\pi^5}{\lambda^4} Z |k|^2 10^{-10} \tag{17}$$

Using the appropriate volume from (3) and the extinction coefficient from (15)

$$\sigma_v = \sigma_r V \frac{K_{er}[Rr]}{\beta_v} \tag{18}$$

and the appropriate area coupled to the rain cell from (4) in

$$\sigma_g = \sigma_o(A_n) , \tag{19}$$

where the magnitude of σ^o depends on the type of surface. We compute the SCR

$$\Delta\sigma_{dB} = \sigma_{v_{dB}} - \sigma_{g_{dB}} \tag{20}$$

where

$$\sigma_{v_{dB}} = 10 \log(\sigma_v) \tag{21}$$

and

$$\sigma_{gdB} = 10 \log(\sigma_{gT}) \tag{22}$$

For the ideal case, the clutter coupled to the rain returns at vertical incidence is negligible. However in practice the surface return from range sidelobes arrives at the receiver at the same instant as the desired rain echo. The sidelobe levels with a raised $\cos^2$ window are low, with the first side lobe about 21 dB down. Due to the very large magnitude of the surface clutter and due to the fact that the side lobes fall too slowly (see Fig. 5), almost all rain cells have significant clutter coupled to them. From Fig. 5 it is seen that the magnitude of the sidelobes that are coupled to the surface echo depends on the cell for which the calculations are made. Further, even the sidelobes that are coupled to the ground return change in magnitude with the cell under consideration. To account for this, using (9) and the cell number under consideration, it is possible to obtain the exact number of side lobes coupled to the ground. Their magnitude $Sl_{dB}(n)$, can be obtained from the figure. The weighted clutter coupled to the cell under consideration is obtained as

$$\sigma_{gT}\ (R_r) = \sum_n \sigma_g\ (R_r, n)\ 10^{0.1\ Sl_{dB}(n)} \tag{23}$$

where

$$\sigma_g(R_r, n) = \frac{A_n\ K_{er}[Rr]\ 10^{0.1\ \sigma_o}}{\mathbf{B}_v} \tag{24}$$

Using (20) plots of the SCR for various rain thicknesses over ocean are compared with SCR over forest for rain thickness of 1 km at X band (see Fig. 6(a)). Fig. 6(b) shows the comparison between the SCRs obtained using a raised $\cos^2$ window and an ideal $\cos^2$ window over the ocean at X band. Fig, 6(c) and 6(d) show corresponding comparisons at C band. From the figures it is seen that the X-band and C-band SCR with a raised $\cos^2$ window is poor

Values of Parameters in the Relationships
$\kappa_{dB} = \kappa_1 R^b$; (Logarithmic Model) and $\kappa_{dB} = \kappa_1 R$, (Linear Model)

	Logarithmic model[a]				*Linear model*	
	κ_1		b		κ_1	*Comments*[b]
Frequency (GHz)	V	H	V	H		
2.8	0.000459		0.954		—	(1)
7.5	0.00459		1.06		0.00481	(1)
9.4	0.0087		1.10		0.00932	(1)
11.0	0.012	0.014	1.23	1.24	—	(2)
16.0	0.0374		1.10	1.24	0.0403	(1)
18.0	0.053	0.061	1.07	1.10	—	(2)
24.0	0.10	0.11	1.03	1.06	—	(2)
30.0	0.17	0.19	0.98	1.00	—	(2)
34.9	0.225		1.05		0.234	(1)
40.0	0.31	0.38	0.91	0.93	—	(2)
60.0	0.63	0.71	0.81	0.82	—	(2)
69.7	0.729		0.893		—	(1)
80.0	0.86	0.93	0.76	0.77	—	(2)
100.0	1.06	1.15	0.73	0.73	—	(2)

[a] The symbols V and H refer to vertical and horizontal polarizations.
[b] (1) Computed for spherical particles by Crane (1971); (2) computed for oblate spheroidal drops, reported by Harden et al. (1978).

Table.1 The attenuation coefficients at various frequencies may be picked off from here to be used in the relation discussed.

(Lin,1975; Morrison and Cross, 1974)

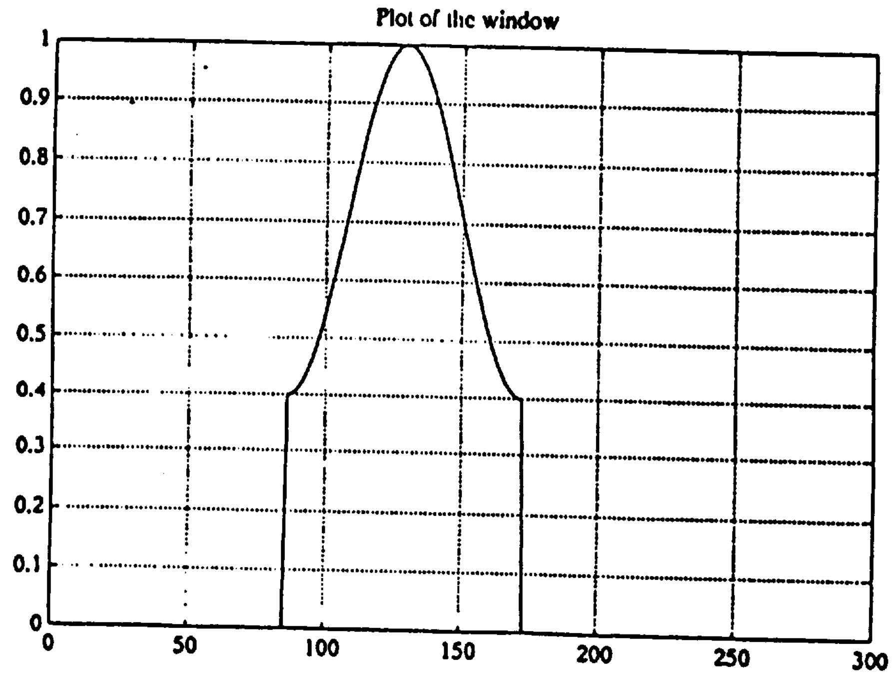

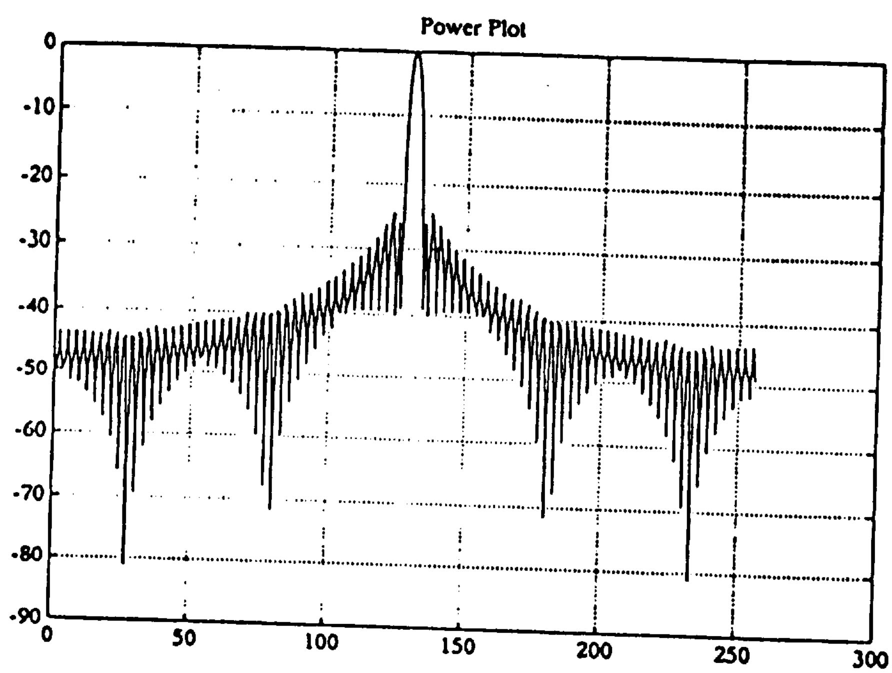

Fig.5 The sidelobe level in dB, due to the use of a raised cos² window with a pedestal of 0.4 for data processing.

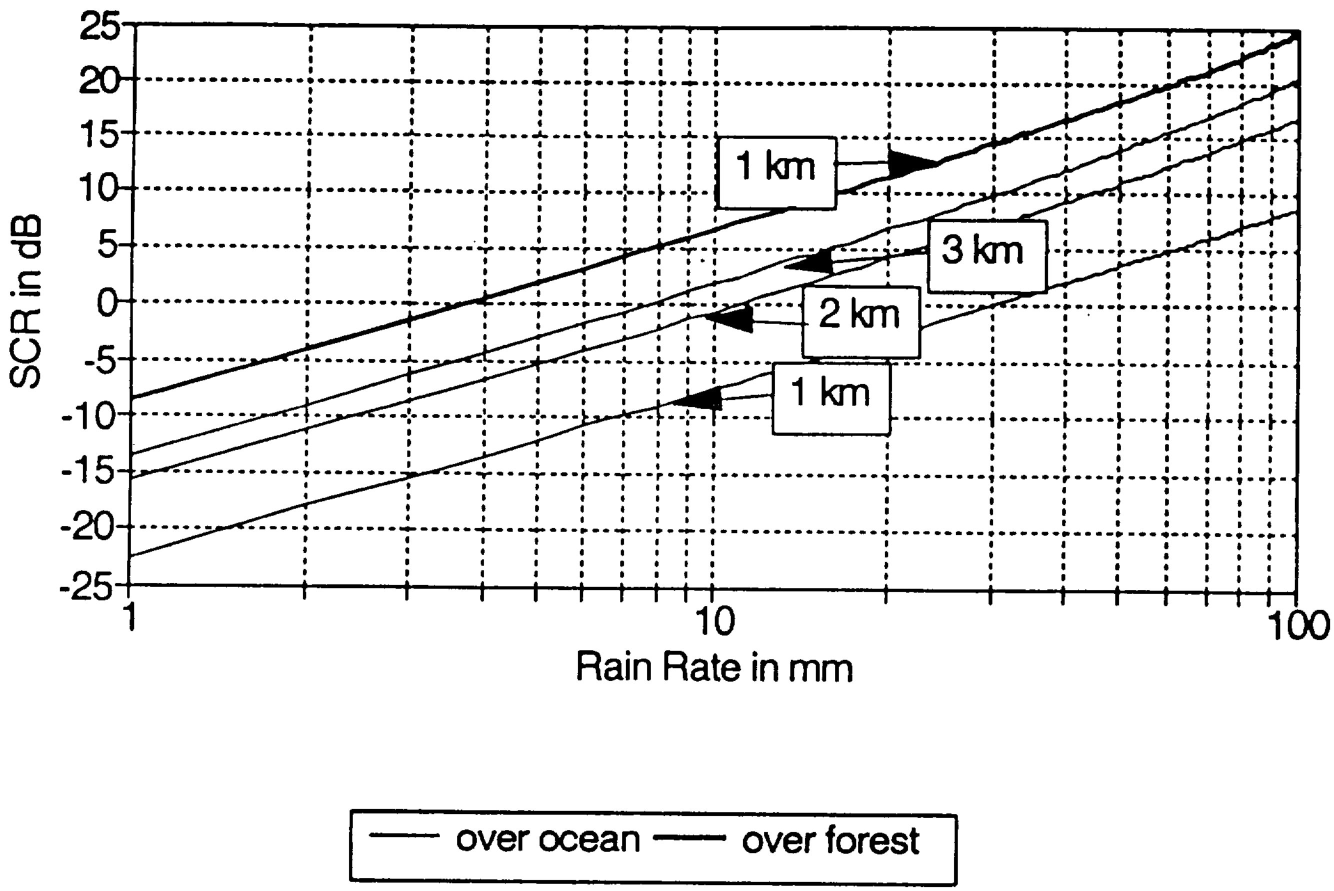

Fig.6a. Plot of X -band SCR in dB vs Rain rate in mm/hr over ocean and over forest for the given rain thickness for raised cos^2 weighting.

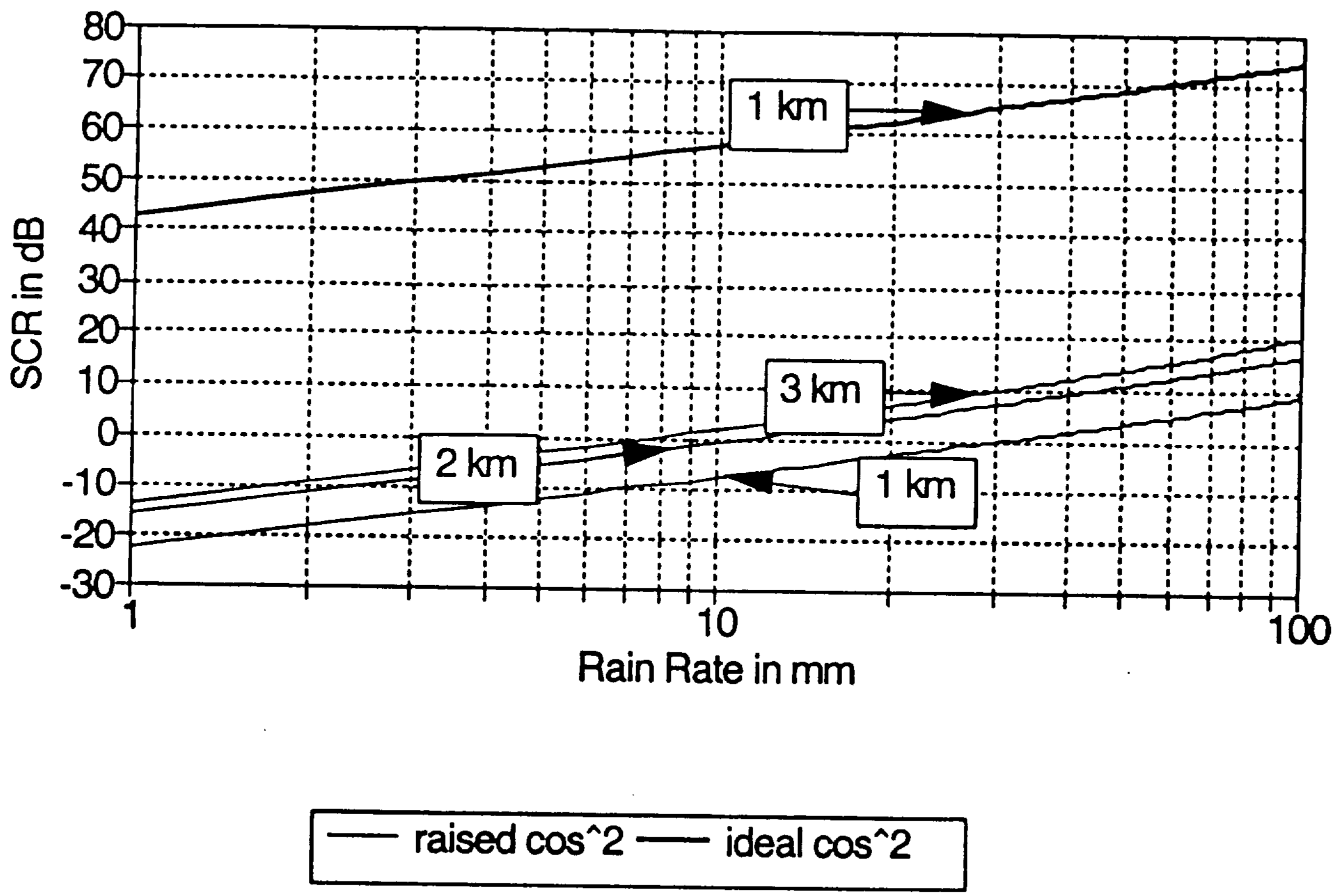

Fig.6b Comparison of the X-band SCR over ocean using raised $\cos^2$ and ideal $\cos^2$ weighting for the given rain thickness.

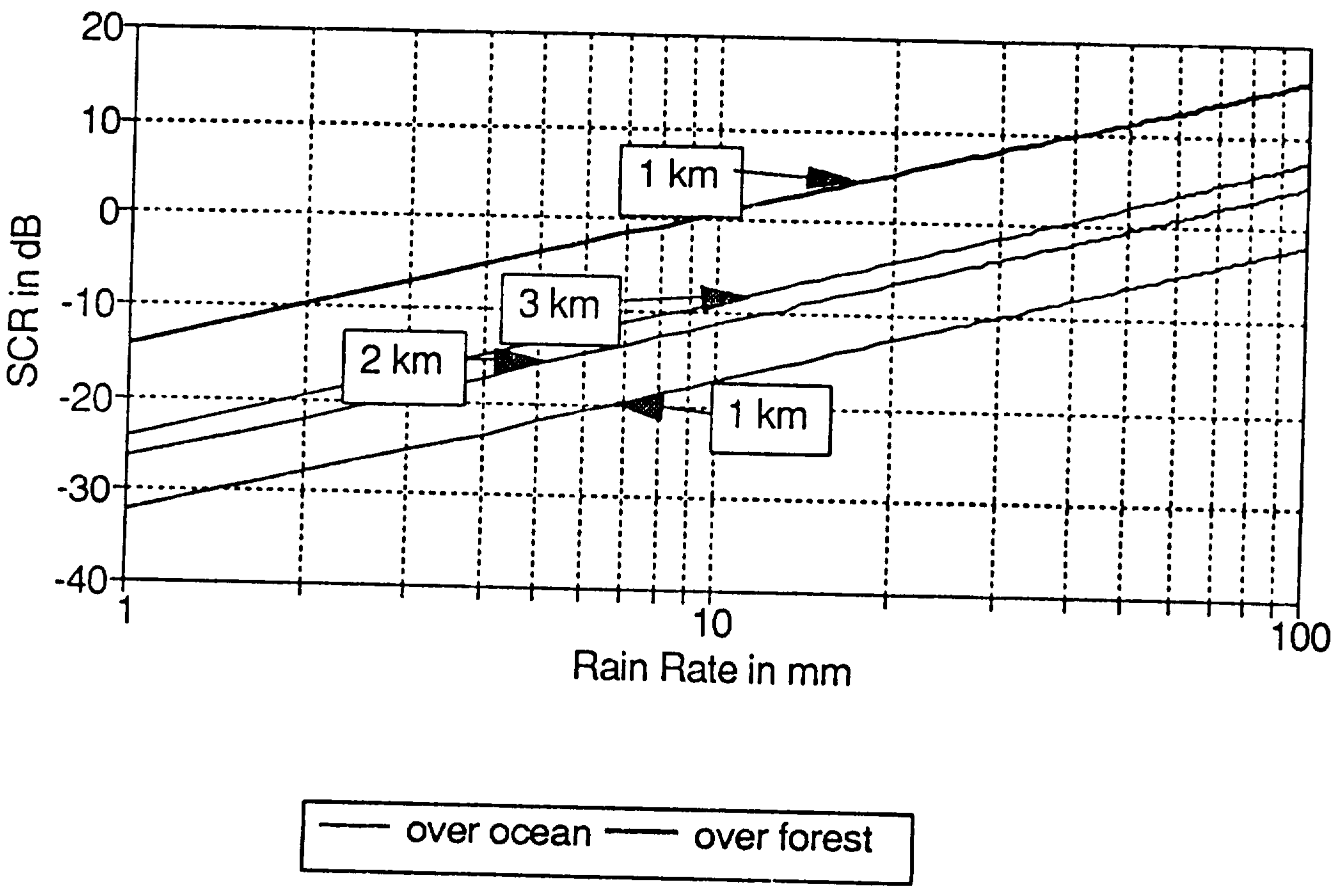

Fig.6c. Plot of C-band SCR in dB vs Rain rate in mm/hr over ocean and over forest for the given rain thickness for raised $\cos^2$ weighting.

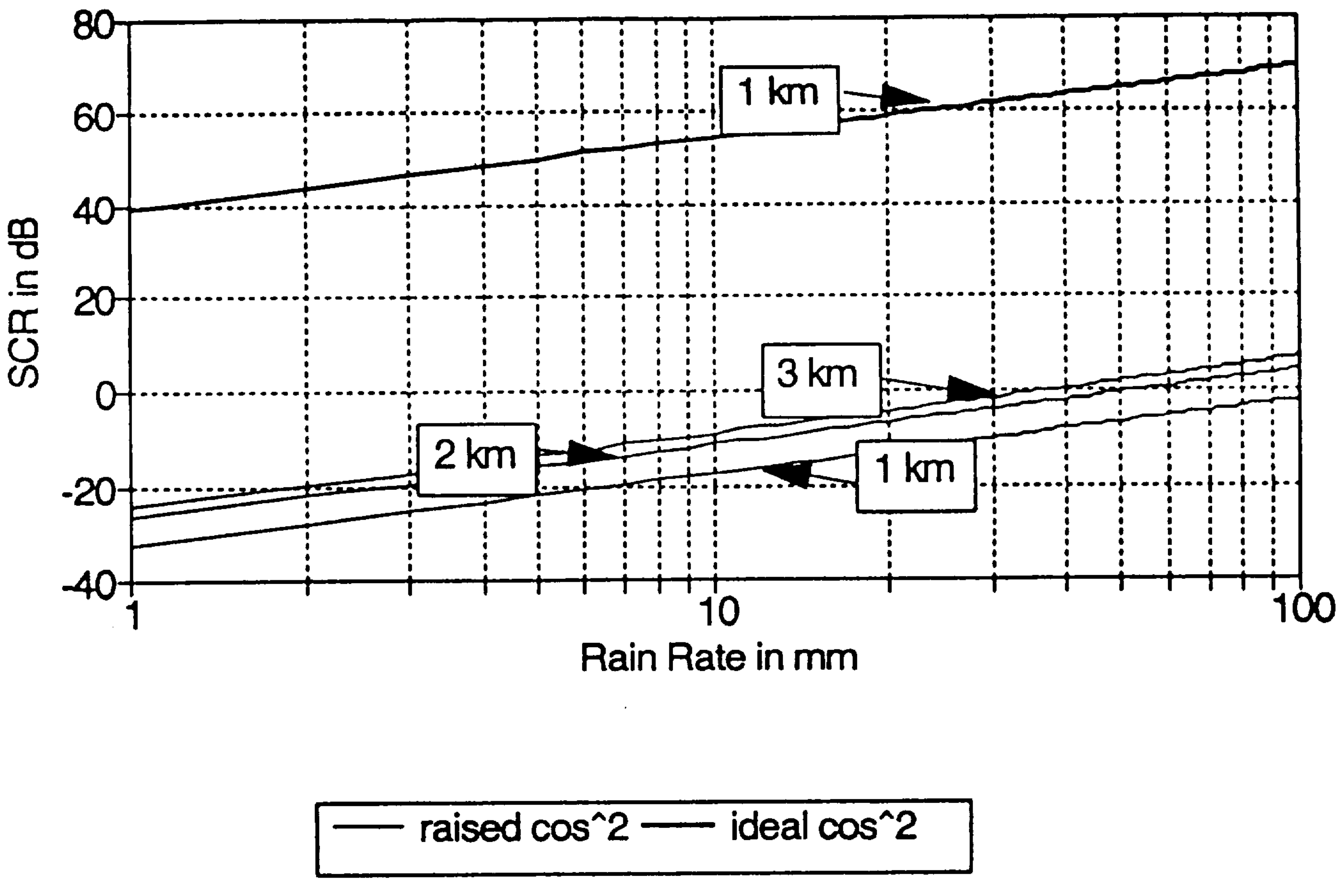

Fig.6d Comparison of the C-band SCR over the ocean for a raised $\cos^2$ and a ideal $\cos^2$ weighting for the given rain thickness.

over the ocean for shallow rain thickness. However over the forest the SCR appears to be reasonable even for shallow rain thickness with a raised $\cos^2$ window. Further for both X and C bands the SCR is expected to be good even for shallow rain thickness over ocean if an ideal $\cos^2$ weighting could be achieved.

6.0 CONCLUSIONS

Though the SAR has a good SNR at all angles of incidence, it has inadequate SCR under most conditions. For the backscatter algorithm to work, the return from rain must have a magnitude greater than the surface return. From the plots it is seen that the SCR (which gives a measure by how much the rain return lies above the ground return) at nadir is very low for small rain rates over oceans (see Fig. 6(a)). This implies that the backscatter method cannot be used over ocean for rain rates < 30 mm for shallow rain thickness using a raised $\cos^2$ weighting. However, the SCR for forest at vertical incidence is adequate for rain rates > 5 mm/hr even for rain thickness of 1 km at X band and > 10 mm/hr at C band. For low rain thickness, measurements over the ocean are not feasible for both vertical incidence and off-vertical incidence except at very high rain rates. However, for rain thickness > 2 km, measurement over ocean at X band for rain rates > 10 mm is possible at nadir. For C band the SCR is very poor even at high rain rates as seen in Fig. 6(b).

Since far-out sidelobes are the problem at vertical incidence, it is suggested that the sidelobe level be reduced by an additional 10 dB during processing so that the experiment may be conducted over the ocean at nadir for shallow rain thickness. Here the absolute level of the sidelobes is not the issue and any weighting function that gives sidelobes which rapidly decrease in magnitude is recommended. Clearly with ideal $\cos^2$ weighing the SCR is expected to be very good even at shallow rain rates (Fig. 6(b), Fig. 6(d)). However, over forest X-band and C-band vertical incidence results are expected to be good even with the present weighting. This does not mean that experiment is feasible over forest at all angles because the clutter return from forest is higher than that of the ocean at incidence angles far from the vertical.

It is believed that the rain retrieval algorithm could work for low rain rates at shallow rain thickness if it is possible to have an independent estimate of the signal and clutter and the clutter alone. By subtracting the average clutter estimate from the average rain signal-plus-clutter estimate it is possible to implement the rain retrieval algorithm. This will be discussed in a separate report.

REFERENCES

Atlas, D. and R.K. Moore, "The measurement of precipitation with the synthetic aperture radar," *Journal of Atmospheric and Oceanic Technology*, vol.4, pp.368-376, 1987.

Battan, L.J., *Radar Observation of the Atmosphere*, University of Chicago Press; Chicago, 1973.

Lin, S.H, "A method for calculating tain attenuation distributions on microwave paths," *Bell Syst. Tech. J.* , 54, pp 1051-1086, 1975.

Morrison, J.A and M. J Cross, "Scattering of a plane Electromagnetic wave by axi-Symmetric rain-drops," *Bell Syst. Tech. J.*, 53 pp 955-1020, 1974

Schroeder, L.C., P.R. Send, J.L. Mitchell, and L.W Jones, "AAFE RADSCAT 13.9 G-Hz measurements and analysis: Wind-speed signature of the ocean," *IEEE J. Ocean. Engr.*, vol OE-10 no.4, pp.346-357, 1985.

House:Norwood, MA, 1981.

Ulaby, F.T., R.K. Moore, and A.K. Fung, *Microwave Remote Sensing*, Vol III Artech House:Norwood, MA, 1986.

APPENDIX - I

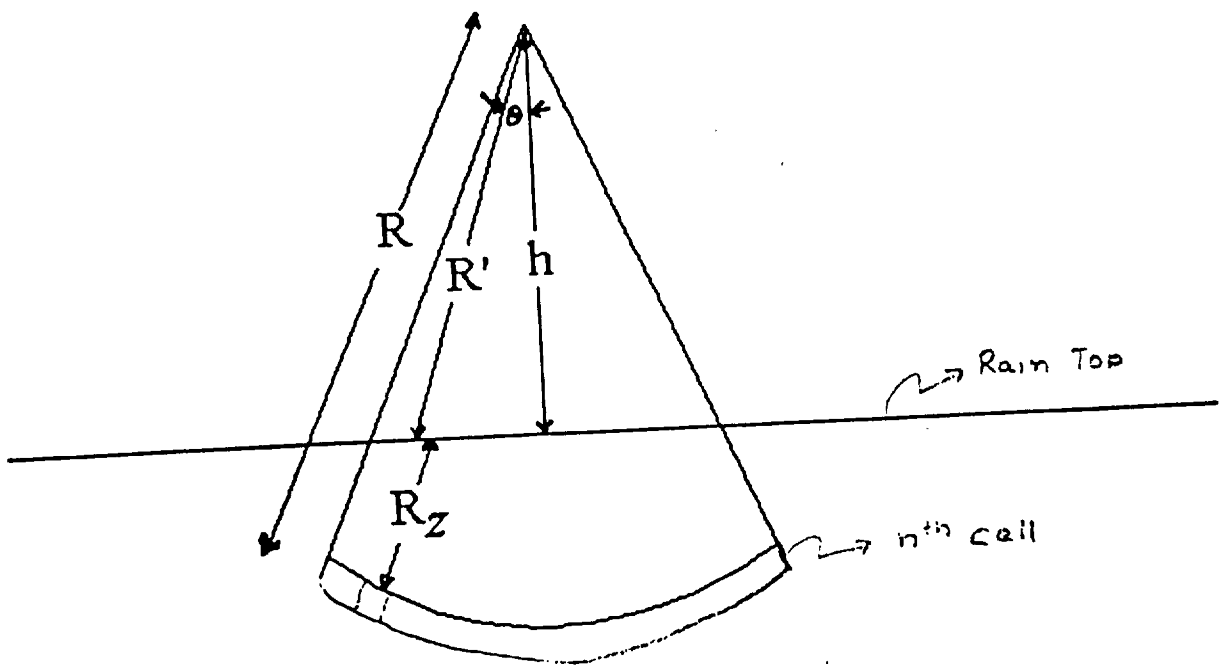

Fig.a The geometry of the pulse volume showing that the signal from different parts of the pulse volume passes through different rain thickness

From Fig. a it is seen that the volume occupied by the rain above each rain cell changes from one end of the cell to the other. This is due to the fact that pulse volume is curved where as the rain top is not. Hence the signal from the cell edge suffers less attenuation than the center. To account for this it is necessary to integrate the attenuation over the entire pulse volume. Here it is necessary to make the assumption that the cell has constant attenuation in the azimuth direction. The rain returns involve

$$\sigma_v \frac{\pi}{4} \beta_h r_R \int_{-\frac{\beta_v}{2}}^{\frac{\beta_v}{2}} R^2 e^{-\alpha R_z} dR \qquad (a)$$

we may write R = (h + n r_R) where n is the cell number under consideration, r_R is the range resolution and h is the height to the shuttle from the rain top. In order to account for the variation of the distance travelled by the signal in the rain volume it is assumed that the beamwidth can be divided into number of small angles. From Fig. a

$$R_z = h + n r_R - \frac{h}{\cos\theta} \qquad (b)$$

where θ varies from - βv/2 to βv/2. Substituting (b) in (a) for the rain returns we have

$$\sigma_v \frac{\pi}{4} \beta_h r_R (h + n r_R)^2 \int_{-\frac{\beta_v}{2}}^{\frac{\beta_v}{2}} e^{-\alpha\left(\frac{h(\cos\theta - 1)}{\cos\theta} + n r_R\right)} d\theta \qquad (c)$$

Here the attenuation coefficient

$$k_{er} = \int_{-\frac{\beta_v}{2}}^{\frac{\beta_v}{2}} e^{-\alpha\left(\frac{h(\cos\theta - 1)}{\cos\theta} + n r_R\right)} d\theta \qquad (d)$$